Mechanism of Interfacial Mass Transfer in Membrane Transport

THOMAS G. KAUFMANN and EDWARD F. LEONARD

Columbia University, New York

Dialysis of binary aqueous solutions of several sugars through a cellophane membrane was studied in a stirred batch dialyzer. Sherwood numbers describing mass transfer resistance in the fluid adjacent to the membrane were determined as a function of the corresponding Reynolds and Schmidt numbers. The results establish a reproducible environment for membrane testing in which a known controllable and small interfacial resistance is placed in series with that of the membrane. The results are also shown to support, for this geometry, the postulation of a third power relationship between eddy diffusivity and dimensionless distance from the phase boundary as well as the Sherwood-Ryan nondimensionalization of this distance.

The increased use of membranes as mediators of interfacial mass transfer has provided yet another incentive for the study of turbulent mass transfer at solid-liquid interfaces. In order to determine mass transfer resistances within membranes, in the design of plant and pilot plant-scale devices and in the conduct of laboratory experiments, knowledge of interfacial mass transfer coefficients is needed and the adequacy of present knowledge is tested, particularly when turbulent flow conditions are encountered or desired. The results reported here were obtained as part of a study of transport near and within cellophane membranes through which binary solutions of one of several sugars in water were being transferred. The principal mechanism of transport was dialysis: a relative movement of species in response to concentration differences. The inseparable presence of volume transport was recognized, however, and certain corrections were made for it. The results of the intramembrane transport studies are described in a separate paper (*10*).

Membrane evaluation has for the most part been conducted by chemists and biological scientists and the literature expresses relatively little concern for the difference between overall resistance to transport between phases, and that resistance inherent to the membrane (*4, 15, 16*). Some prior studies have been reported in which the presence of interfacial resistances was recognized and steps were taken to measure and control them (*3, 11*). However, firm establishment of how interfacial resistances vary with diffusional and hydrodynamic parameters in a convenient and desirable environment for testing membranes has not yet been achieved. Since it is important to emphasize intramembrane transport, turbulence is often introduced to minimize interfacial resistances and to insure known concentrations at the membrane surfaces. When the turbulent interfacial resistances are known, in terms of diffusional and hydrodynamic parameters, accurate measurement of transport across a membrane under a given condition is reduced from many experiments to one.

A convenient and commonly used controlled environment for measuring membrane resistances is shown in Figure 1: a pair of identical, enclosed, stirred, cylindrical chambers sharing a circular boundary across which the membrane is interposed. When different initial concentrations are established in the chambers, the approach to equilibrium may be followed to yield an overall mass transfer coefficient. When the solutions in the chambers have nearly identical physical and transport properties, and when care is taken to design and operate each chamber identically, the interfacial transport processes in each half of the device may be jointly considered, and each may be assumed to possess the same characteristic resistance which is one half of the total interfacial resistance.

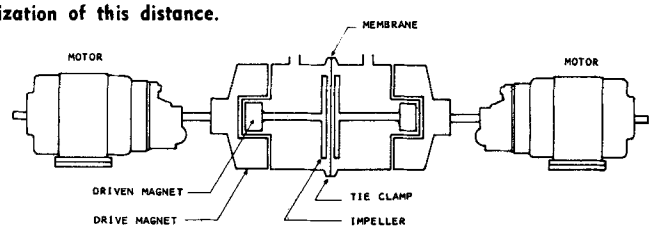

Fig. 1. Basic configuration of batch dialyzer.

Studies of transport to the stationary surfaces of stirred vessels clearly relate to the proposed testing environment, but are relatively few in number when the vessels are closed and unbaffled even though the latter condition gives greater transfer than does baffling (*8*). Hence there is a general need for further understanding of transport in this configuration, apart from the concern with membrane studies.

Finally, when one considers the problem of mass transfer between solids and liquids in its most general sense, there still does not exist a clear reconciliation of macroscopic determinations of the $N_{Sh} - N_{Re} - N_{Sch}$ relationship and the microscopic events near the interface which determine these relationships.

This paper is directed to three ends: establishing a firm understanding of an environment of membrane testing that is easy to use and has a low, predictable fluid film resistance; enhancing the understanding of transport between fluids and stationary surfaces in closed, unbaffled stirred vessels and providing additional experimental results to help resolve uncertainties about the mechanism of turbulent interfacial transport in a geometrical situation which complements previous studies.

INTERFACIAL TRANSPORT IN STIRRED VESSELS

Working equations and most correlations of experimental results for turbulent interfacial transport in many different geometries take the form of

$$N_{Sh} = \gamma N_{Sch}{}^{b} N_{Re}{}^{c} \qquad (1)$$

In a configuration close to that investigated in this work, Holmes et al. (*6*) studied a diffusion cell in which the interchamber barrier was a porous glass disk and the stirrers were magnetized bars at the respective bottoms of two cylindrical cells whose axes were vertical; they obtained values of 0.38 for the exponent b and 0.79 for c. Marangozis and Johnson (*13*) concluded that many types of interfacial transport data could be grouped and then fit by setting b equal to 0.33 and c equal to 0.70. For their own studies of the dissolution of cast solids from the bottom of a baffled, agitated vessel, they obtained an exponent b of 0.33 and an exponent c of 0.65. Similar re-

T. G. Kaufmann is with Esso Research and Engineering Company, Florham Park, New Jersey.

sults are obtained for so seemingly different a situation as duct flow, where the exponent b has most often been taken as 0.25 or 0.33 while the exponent c has been taken as 0.8 and 0.9 at high Reynolds numbers [that is, as the Sherwood number, N_{Sh} has been taken to depend on $N_{Re} \cdot f$ or $N_{Re} \cdot f^{1/2}$ (18)]. That results for such different geometries are so similar can be rationalized by observing and relating three facts: turbulent interfacial resistances are in fact concentrated quite close to phase boundaries; the radius of curvature of most phase boundaries is much larger than the thickness of the zone in which most of the interfacial resistance is concentrated so that the phase boundary can be regarded as a plane; to a good approximation some universal function seems to describe the transition from stasis at the boundary to bulk turbulence.

Macroscopic studies, especially when they include frictional measurements, can contribute to the current critical re-examination of the relationship between correlations, such as Equation (1), and analogies on the one hand, and consideration of the microscopic descriptions of velocity profiles and transport near phase boundaries on the other hand. The present results, as those just cited, lend no support to the simple film theory (which presumes N_{Sh} independent of N_{Sch}) nor to the unadorned penetration theory (2) (N_{Sh} proportional to $N_{Sch}^{0.5}$). The presence of a laminar boundary layer as the controlling resistance in turbulent systems also seems unlikely since most of these solutions, including Levich's closely related analysis of mass transfer through a laminar boundary layer on a dissolving rotating disk (12), indicate that N_{Sh} is proportional to $N_{Re}^{0.5}$; a dependence supported neither by the extant literature nor this study.

Turbulent boundary-layer theory has received increasing but not unequivocal support as a vehicle for relating macroscopic correlations to processes occurring at the microscale. Within turbulent boundary-layer theory, two choices determine the exponents for f [and thus for N_{Re} since $f = f(N_{Re})$] and N_{Sch} in the resultant working, asymptotic, macroscopic relations: the way in which distance y, measured from the boundary, is nondimensionalized and the exponent chosen for the power law assumed to relate the eddy transport coefficient, ϵ, to dimensionless y (7, 20). Sherwood and Ryan (19) show that when the dimensionless form of y is taken as von Karman's y^+, one obtains

$$\epsilon/\nu = \phi_1(y^+) \tag{2}$$

where

$$y^+ = \frac{y}{\nu}\sqrt{\frac{\tau_o}{\rho}} \tag{3}$$

which leads to

$$N_{Sh} = \psi_1(N_{Sch}) N_{Re} \sqrt{f/2} \tag{4}$$

whereas if one nondimensionalizes y in the form of y^{++}, there results

$$\epsilon/\nu = \phi_2(y^{++}) \tag{5}$$

where

$$y^{++} = \frac{y\tau_o}{\nu\rho v} \tag{6}$$

which gives the macroscopic relation

$$N_{Sh} = \psi_2(N_{Sch}) N_{Re} f/2 \tag{7}$$

Equation (7) is in agreement with the Reynolds number dependence found in many macroscopic studies.

As numerous authors have shown, the second choice, the power chosen for the $\epsilon/\nu - y^+$ or y^{++} relationship is reciprocal to the power found for N_{Sch} in the macroscopic relation. Powers of three and four have been proposed and macroscopic studies have been claimed to correlate with exponents for N_{Sch} both 1/4 and 1/3 (7). The present study helps to determine how these choices should be made for the stirred geometry in which the measurements described below were made.

EXPERIMENTAL PROCEDURE

The transport measurements were made in a batch dialyzer. Its essential features are shown in Figure 1; additional details are given in Figure 2. Each chamber, approximately 3 in. in diameter and 2.44 in. in length, was equipped with a heater, volume compensating plunger, and axially mounted turbine type of agitator. One chamber was also equipped with a thermistor temperature probe. Both agitators were driven through magnetic couplings by 1/50 hp thyratron-controlled, variable-speed motors, and were comprised of four flat blades spaced 90 deg. apart. The tip-to-tip distance of opposite blades was 2.82 in.; the blades were 1/16 in. thick and 1/4 in. wide. The nearest plane of rotation was 0.078 in. from the membrane surface. Further details of the dialyzer design, including an assembly drawing, are given by Kaufmann (9).

In each experimental run a fixed stirring speed for each chamber was established and maintained using a calibrated stroboscope. The concentration of the sugar under study (glucose, raffinose, or sucrose) was determined as a function of time in the chamber which had been initially charged with 0.1 M sugar solution, by noting the freezing point depression of the solution using an Industrial Instruments Co. Model CR-1 Cryoscope. Concentrations in the second chamber, charged initially with 0.005M solution, were determined by mass balance. This analytical scheme was used because the cryoscope behaved most reliably and accurately when concentrations in the range of those maintained in the first chamber were analyzed.

Fifty two experimental conditions, involving stirring speeds of 46 to 500 rev./min., three different sugars, and three temperatures, 27°, 37°, and 47°C., were examined with duplicate runs. These were resolved into seven sets of results with only the stirring speed varying, (runs with raffinose were only made at 37°C.).

In order to clarify the variation of interfacial resistance with hydrodynamic conditions, measurements were made of the torque-speed relationship for this system, by using a geometric replica of one dialyzer chamber mounted vertically on a torque table. The starting torque for the system was about 0.009 in oz. The system sensitivity was such that the speed associated with a given torque could be determined to within 1%. A range of Reynolds numbers ($d^2\Omega\rho/\mu$) from 29 to 452,000 was covered by using water, glycerol-water, and sucrose-water solutions.

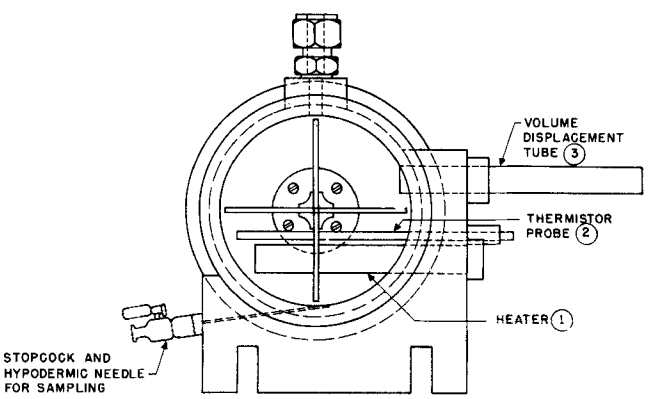

Fig. 2. View from membrane surface of one batch dialyzer chamber. Heater (1) is controlled by signal from thermistor probe (2). Volume displacement tube (3) keeps liquid level constant and prevents air entrainment when samples are removed.

ANALYSIS OF RESULTS

The dialysis coefficient, K, was defined by the equation

$$-\frac{dN^{II}}{dt} = \frac{dN^{I}}{dt} = KA\,(C^{II} - C^{I}) \qquad (8)$$

A small but significant concomitant volume transport was unavoidable and was characterized as follows:

$$\frac{dV^{II}}{dt} = -\frac{dV^{I}}{dt} = LA(C^{II} - C^{I}) \qquad (9)$$

Note, that the term L is related to the cross phenomenological coefficient L_{pD} (*10*). Using for each chamber the relationship

$$\frac{dN^{i}}{dt} = \frac{d(V^{i}C^{i})}{dt} = V^{i}\frac{dC^{i}}{dt} + C^{i}\frac{dV^{i}}{dt} \qquad (10)$$

and assuming that even though V's and C's are changing the quantities, $(1/V^{I} + 1/V^{II})$, and $(C^{I}/V^{I} + C^{II}/V^{II})$ are constant (an assumption good in all cases to better than 1%) one may obtain the integrated equation

$$\ln\frac{(C^{II} - C^{I})_o}{(C^{II} - C^{I})_\tau} = [KA(1/V^{I} + 1/V^{II}) + LA(C^{I}/V^{I} + C^{II}/V^{II})]\tau \qquad (11)$$

Plots of the left-hand side of Equation (11) vs. time, τ, yielded straight lines from whose slopes K could be determined if L were known, A and the V's being measurable. The quantity L was determined in separate experiments (*9, 10*); the contribution of the term in which it appears to the right side of Equation (11) ranged from less than 1% to about 5%.

For each set, K^{-1} was plotted against stirrer speed, n, raised to a power a, adapting the suggestion first made by Wilson (*21*) for separating wall and fouling coefficients from film coefficients in heat exchanger tests. The power which best fit each set was determined as that which minimized the sum of squares of the y deviations. Table 1 summarizes the results.

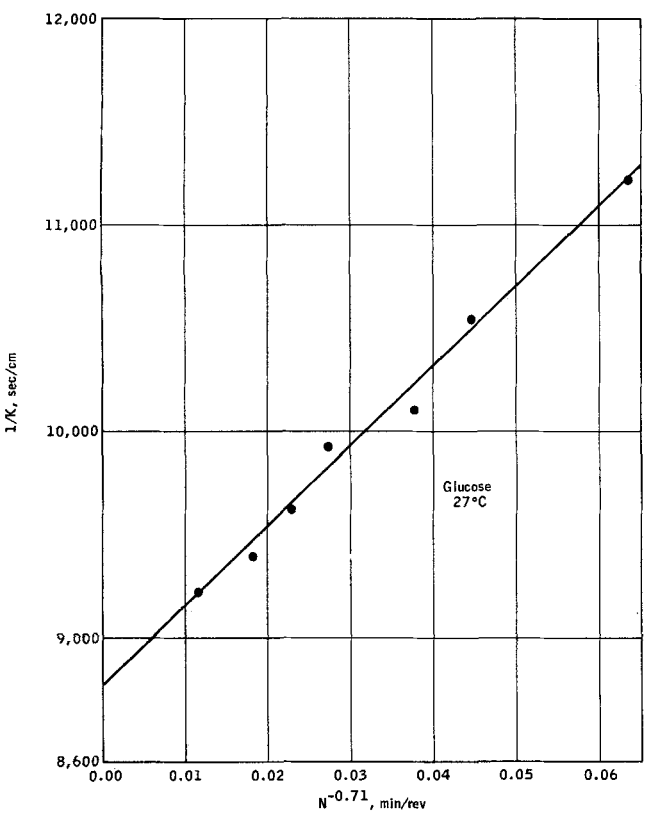

Fig. 3. Determination of overall dialysis coefficient.

TABLE 1. BEST POWERS OF n

Solute:	Glucose	Surcrose	Raffinose
27°C.	0.71	0.82	—
37°C.	0.70	0.75	0.73
47°C.	0.62	0.70	—

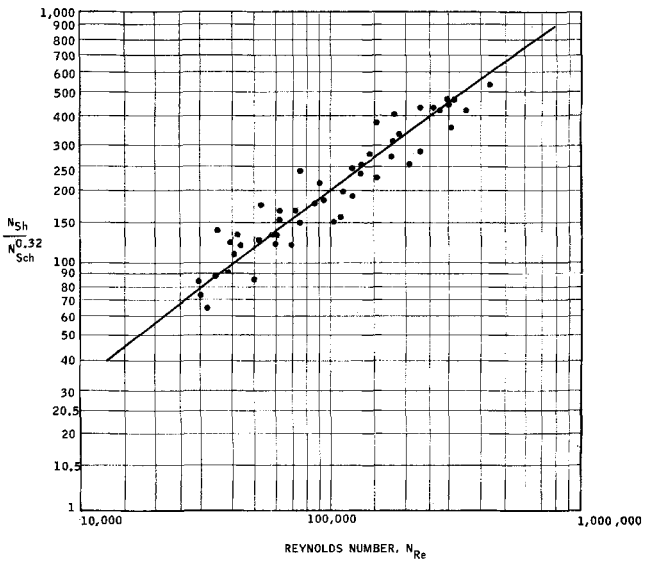

Fig. 4. Dimensionless correlation for the interfacial mass transfer coefficient.

The temperature dependence of a, as implied by Table 1, is considered fortuitous. A typical Wilson plot for one set of results (glucose, 27°C.) is shown in Figure 3. Once the y-axis intercept of a Wilson plot, $1/k_m$, has been obtained, the phase boundary mass transfer coefficients k_p can be obtained from the relationship

$$k_p = 2/(1/K - 1/k_m) \qquad (12)$$

To the fifty-two values of k_p so obtained eight k_p's were added determined by Odian (*14*) for urea in dilute water solution at 37°C., covering a similar speed range in an internally identical apparatus. No volume correction was applied in the analysis of the urea runs since applicable L values were not available. However, this correction is probably negligible for urea. The 60 k_p's represent a range of N_{Sch} $(=\mu/\rho D)$ from 387 to 1,622, and a range of $N_{Re}(=d^2\Omega p/\mu)$ from 23,500 to 440,000.

The k_p's were expressed as $N_{Sh}(=k_p d/D)$ and presumed to fit an equation of the form

$$\ln N_{Sh} = a + b \ln N_{Sch} + c \ln N_{Re} \qquad (13)$$

The constants a, b, and c were found by multiple regres-

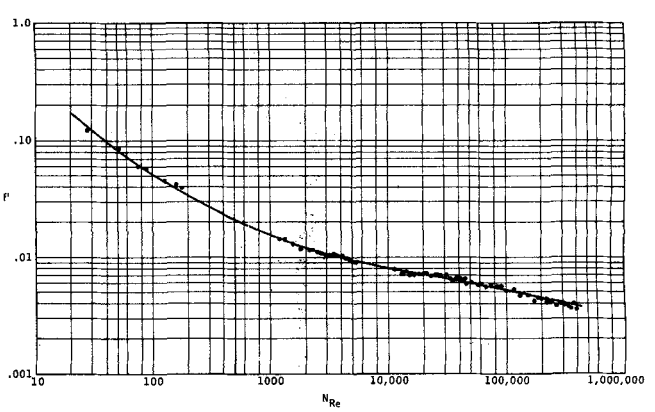

Fig. 5. Friction factor vs. Reynolds number.

sion analysis giving the equation

$$\left(\frac{k_p d}{D}\right) = 0.105\left(\frac{\mu}{\rho D}\right)^{0.32}\left(\frac{d^2\Omega\rho}{\mu}\right)^{0.68} \quad (14)$$

which is plotted with the experimental results in Figure 4. The tabulated data are presented in (9).

Torque speed measurements were converted to the friction factor f'

$$f' = \frac{32T}{\rho\Omega^2 d^5} \quad (15)$$

which is of the form suggested by Brown et al (1), except that impeller diameter d has been substituted for tank diameter, their ratio being 0.958. Figure 5 is a plot of f' vs. N_{Re}.

DISCUSSION

Values of the interfacial transport coefficients obtained in this work are not directly comparable to other published studies, because of geometric differences near the transport surface. However, the variation of N_{Sh} with N_{Sch} and N_{Re} can be examined. The exponent 0.32 corresponds with Maragozis and Johnson's 0.33 and differs somewhat from Holmes et al.'s 0.38; it accords with a third power variation of ϵ with dimenionless y. The exponent 0.68 is near Maragozis and Johnson's 0.65 but significantly below Holmes' et al. 0.79. Their agitators, however, were far removed from the phase boundary (6).

The transport results and friction factor measurements may be used together to determine which choices within turbulent boundary-layer theory are in closest accord with them.

We first consider transport from the membrane surface on the locus of points described by radius r. The flux through the boundary layer is assumed to be entirely in the axial direction, y, and steady:

$$J = -\nu\left(\frac{1}{N_{Sch}} + \frac{\epsilon}{\nu}\right)\frac{dc}{dy} \quad (16)$$

where $y = 0$ at the surface and extends perpendicular to the surface into the fluid. If ϵ is taken as

$$\epsilon = \kappa\nu\,(y^{++})^3 \quad (17)$$

then

$$\epsilon = \kappa\nu\left(\frac{y\tau_o}{\nu\rho v}\right)^3 \quad (18)$$

By combining (16) and (18) and rearranging we obtain

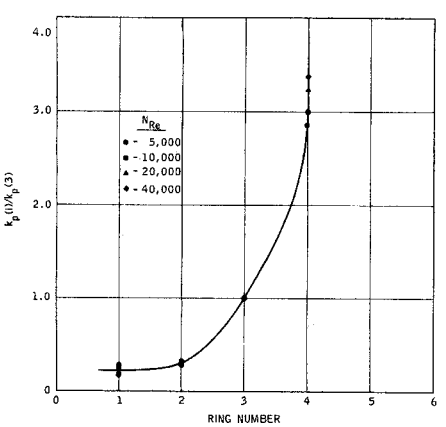

Fig. 6. Variation of local interfacial mass transfer coefficient with radial position. Ordinate is k_p of the i^{th} ring divided by k_p of ring 3 of the same N_{Re} (8).

$$-\frac{dc}{J} = \frac{dy}{D[1 + \kappa N_{Sch}(y^{++})^3]} \quad (19)$$

If J is recognized as necessarily constant and boundary conditions are

$$c = c_o \text{ at } y = 0$$
$$c = c_b \text{ as } y \to \infty$$

then Equation (19) may be integrated to yield

$$\frac{D}{k_p} = \frac{\nu\rho v}{\tau_o(\kappa N_{Sch})^{1/3}}\int_o^\infty \frac{dx}{1 + x^3} \quad (20)$$

where

$$x = y^{++}(\kappa N_{Sch})^{1/3} \quad (21)$$

which on further rearrangement and evaluation of the definite integral gives

$$N_{Sh}(r) = \frac{3\sqrt{3}}{2\pi}\kappa^{1/3}\left(\frac{\tau_o}{v}\right)\left(\frac{d}{\nu\rho}\right)N_{Sch}^{1/3} \quad (22)$$

The factors in the N_{Sh} expression which permit it to vary with radius are τ_o and v. However, if the radial distributions of τ_o and v do not depend on N_{Re}, that is if

$$\tau_o(r,N_{Re}) = Q_\tau(N_{Re})S_\tau(r) \quad (23)$$

$$v(r,N_{Re}) = Q_v(N_{Re})S_v(r) \quad (24)$$

then the dependence of the overall N_{Sh} on f and N_{Re} may be determined. The data of Johnson and Huang for the dissolution of solid rings from the bottom of an unbaffled stirred tank suggests that the radial distribution of N_{Sh} is in fact not strongly dependent on N_{Re}. Figure 6 shows a plot of normalized k_p's vs. radius at several N_{Re}'s covering the range of their study. (The coefficients of their Table 4 were used for these calculations.) We judge that the greater diameter and proximity to the transport surface of the turbine used in this study would further reduce the variation of the radial dependence of N_{Sh} with N_{Re} to be expected here. This evidence supports the contention that the radial distribution of τ_o/v is independent of N_{Re}; it is, however, also necessary to assume that the radial distribution of τ_o itself is independent of N_{Re}. These assumptions are of the equivalents of Equations (23) and (24). By using the latter assumption, one has for the shaft torque T the following:

$$T = Q_\tau\int_o^R rS_\tau(r)2\pi r dr \quad (25)$$

$$T = Q_\tau R^3\int_o^1 \xi S_\tau(\xi)2\pi\xi d\xi \quad (26)$$

$$= Q_\tau R^3\beta$$

If we choose to associate the units of τ_o with Q_τ, then the integral of (26) is a dimensionless coefficient β, which is independent of N_{Re} and N_{Sch}. For the friction factor, one may now write

$$f' = \frac{\beta' Q_\tau}{\rho d^2\Omega^2} \quad (27)$$

One can also obtain an expression for N_{Sh} in terms of $N_{Sh}(r)$

$$N_{Sh} = \left(\frac{3\sqrt{3}}{\pi}\kappa^{1/3}\right)\left(\frac{Q_\tau}{Q_v}\right)\left(\frac{d}{\nu\rho}\right)N_{Sch}^{1/3}\int_o^1 \frac{S_\tau(\xi)}{S_v(\xi)}\xi d\xi \quad (28)$$

by substituting Equations (23) and (24) into (22) after normalization and integration.

If we choose to associate the units of v with Q_v, then the integral of (28) is a dimensionless coefficient α which is independent of N_{Re} and N_{Sch} such as

$$N_{Sh} = \alpha' \left(\frac{Q_\tau}{Q_v}\right)\left(\frac{d}{\nu\rho}\right) N_{Sch}^{1/3} \qquad (29)$$

Combining (27) with (29) and noting that (24) requires that Q_v be proportional to $R\Omega$ we get

$$N_{Sh} = \gamma N_{Sch}^{1/3} N_{Re} f \qquad (30)$$

where γ is a dimensionless constant independent of N_{Re} and N_{Sch}. In the present study f was found to be proportional to $N_{Re}^{-0.22}$ over the range of measurement of transport coefficients. Thus, Equation (30) predicts that N_{Sh} should be proportional to $N_{Re}^{0.78}$, whereas the experimental results suggest that the proportionality should be to $N_{Re}^{0.68}$, a discrepancy of 14.7%. Had the y^+ nondimensionalization been used, the predicted proportionality would be to $N_{Re}^{0.89}$ with a correspondingly larger discrepancy. The 14.7% difference is thought to arise from three sources: uncertainty of the transport results, incomplete interpretation of the frictional measurement, and variation of the functions S_v and S_τ with N_{Re}. Since the best exponent of the Wilson plot was found to be 0.72 whereas the velocity exponent of the final correlation is 0.68, there is an uncertainty of 0.04 units in the transport results themselves. Also, while the principal surface on which torque is developed is undoubtedly the transport surface, f is calculated from the drag observed on the entire wetted surface of the vessel; thus the measured f varies only approximately in the way that f (computed from forces) acting only on the transport surface would vary. Finally, as has been noted, S_v and S_τ are only approximately independent of N_{Re}. Within the limitations imposed by the approximations, the system does appear to conform to the Sherwood-Ryan modification of transport theory for turbulent boundary layers with a third power $\epsilon - y^{++}$ relationship; the system would not conform as well to other proposed forms of turbulent boundary-layer theory, to laminar boundary-layer theory, or to penetration theory.

ACKNOWLEDGMENT

The authors are indebted to R. E. Reiss for designing the torque table and obtaining the frictional data reported here, and to George Trost and Frank Lech who helped design and build the batch dialyzer. This batch dialyzer is a direct descendent of a design developed by L. W. Bluemle, Jr., and built by Charles Gobel of the University of Pennsylvania, and made available to us long before the development of the batch dialyzer described here.

NOTATION

A = membrane area, sq.cm.
a = exponent of stirrer speed, dimensionless
c = concentration, moles/cc.
d = impeller diameter, cm.
D = molecular diffusion coefficient, sq.cm./sec.
f' = friction factor, dimensionless
J = time-averaged diffusion flux, moles/sq.cm. sec.
K = overall dialysis coefficient, cm./sec.
k_m = membrane permeability coefficient, cm./sec.
k_p = interfacial mass transfer coefficient, cm./sec.
L = coefficient defined by Equation (9)
N = moles
n = stirrer speed, rev./min.
N_{Re} = Reynolds number, $d^2\Omega\rho/\mu$
N_{Sch} = Schmidt number, $\mu/\rho D$
N_{Sh} = Sherwood number, $k_p d/D$
Q_v = function defined by Equation (24)
Q_τ = function defined by Equation (23)
r = radial distance, cm.
R = membrane radius, cm.
S_v = function defined by Equation (24)
S_τ = function defined by Equation (23)
T = shaft torque, g. sq.cm./sq.sec.
V = volume, cc.
v = velocity, cm./sec.
x = $y^{++}(N_{Sch})^{1/3}$, dimensionless
y = distance from membrane surface, cm.
y^+ = dimensionless distance defined by Equation (3)
y^{++} = dimensionless distance defined by Equation (6)

Greek Letters

α = dimensionless coefficient defined by Equation (28)
α' = dimensionless coefficient defined by Equation (29)
β = dimensionless coefficient defined by Equation (26)
β' = dimensionless coefficient defined by Equation (27)
γ = dimensionless coefficient defined by Equation (30)
ϵ = eddy diffusivity, sq.cm./sec.
κ = constants defined by Equation (17)
μ = viscosity, g./sec. cm.
ν = kinematic viscosity, sq.cm./sec.
ξ = dimensionless distance, r/R
ρ = density, g./cc.
τ_o = shear stress at the surface, g./cm. sq.sec.
τ = time, sec.
ϕ = ( ) function of
Ω = angular velocity, rad./sec.

Superscripts

I = compartment 1
II = compartment 2

Subscripts

b = main fluid body
o = phase boundary

LITERATURE CITED

1. Brown, G. G., et al. "Unit Operations," Wiley, New York (1950).
2. Danckwerts, P. V., *Ind. Eng. Chem.*, **43**, 1460 (1951).
3. Driessen, R. S., MS thesis, Univ. Pa., Philadelphia (1957).
4. Durbin, R. P., *J. Gen. Physiol.*, **44**, 315 (1961).
5. Hanratty, T. J., *AIChE J.*, **2**, 359 (1956).
6. Holmes, J. T., C. R. Wilkie, and D. R. Olander, *J. Phys. Chem.*, **67**, 1469 (1953).
7. Hubbard, D. W. and E. N. Lightfoot, *Ind. Eng. Chem. Fundamentals*, **5**, 370 (1966).
8. Johnson, A. I., and C. J. Huang, *AIChE J.*, **2**, 412 (1956).
9. Kaufmann, T. G., Ph.D. thesis, Columbia Univer., New York (1965).
10. ———, and E. F. Leonard, *AIChE J.*, **14**, 110 (1968).
11. Lane, J. A. and J. W. Riggle, *Chem. Eng. Progr. Symposium Ser. No. 24*, **55**, 127 (1959).
12. Levich, V. G., "Physicochemical Hydrodynamics," Prentice-Hall, Englewood Cliffs, N. J. (1962).
13. Marangozis, J., and A. I. Johnson, *Can. J. Chem. Eng.*, **40**, 231 (1962).
14. Odian, M., MS thesis, Columbia Univer., New York (1964).
15. Pappenheimer, J. E., E. M. Renkin, and L. M. Borrero, *Am. J. Physiol.*, **167**, 13 (1967).
16. Renkin, E. M., *J. Gen. Physiol.*, **38**, 225 (1954).
17. Rozen, A. M., and V. S. Krylov, *Int. Chem. Eng.*, **6**, 429 (1966).
18. Ruckenstein, E., *Chem. Eng. Sci.*, **22**, 474 (1967).
19. Sherwood, T. K., and J. M. Ryan, *ibid.*, **11**, 82 (1958).
20. Vieth, W. R., J. H. Porter, and T. K. Sherwood, *Ind. Eng. Chem. Fundamentals*, **2**, 1)1963).
21. Wilson, E. E., *Trans. Am. Soc. Mech. Eng.*, **37**, 47 (1915).

Manuscript received February 13, 1967; revision received August 10, 1967; paper accepted August 14, 1967. Paper presented at AIChE Houston meeting.